Published February 1, 2017, doi:10.4049/jimmunol.1601471

Loss of CMAH during Human Evolution Primed the Monocyte–Macrophage Lineage toward a More Inflammatory and Phagocytic State

Jonathan J. Okerblom,[*,†,‡] Flavio Schwarz,[*,†,‡] Josh Olson,[§,¶] William Fletes,[*,‖] Syed Raza Ali,[*,§,¶] Paul T. Martin,[#,,††] Christopher K. Glass,[*,†,‡] Victor Nizet,[*,§,¶] and Ajit Varki[*,†,‡]**

Humans and chimpanzees are more sensitive to endotoxin than are mice or monkeys, but any underlying differences in inflammatory physiology have not been fully described or understood. We studied innate immune responses in *Cmah*$^{-/-}$ mice, emulating human loss of the gene encoding production of Neu5Gc, a major cell surface sialic acid. CMP–*N*-acetylneuraminic acid hydroxylase (*CMAH*) loss occurred ∼2–3 million years ago, after the common ancestor of humans and chimpanzees, perhaps contributing to speciation of the genus *Homo*. *Cmah*$^{-/-}$ mice manifested a decreased survival in endotoxemia following bacterial LPS injection. Macrophages from *Cmah*$^{-/-}$ mice secreted more inflammatory cytokines with LPS stimulation and showed more phagocytic activity. Macrophages and whole blood from *Cmah*$^{-/-}$ mice also killed bacteria more effectively. Metabolic reintroduction of Neu5Gc into *Cmah*$^{-/-}$ macrophages suppressed these differences. *Cmah*$^{-/-}$ mice also showed enhanced bacterial clearance during sublethal lung infection. Although monocytes and monocyte-derived macrophages from humans and chimpanzees exhibited marginal differences in LPS responses, human monocyte-derived macrophages killed *Escherichia coli* and ingested *E. coli* BioParticles better. Metabolic reintroduction of Neu5Gc into human macrophages suppressed these differences. Although multiple mechanisms are likely involved, one cause is altered expression of C/EBPβ, a transcription factor affecting macrophage function. Loss of Neu5Gc in *Homo* likely had complex effects on immunity, providing greater capabilities to clear sublethal bacterial challenges, possibly at the cost of endotoxic shock risk. This trade-off may have provided a selective advantage when *Homo* transitioned to butchery using stone tools. The findings may also explain why the *Cmah*$^{-/-}$ state alters severity in mouse models of human disease. ***The Journal of Immunology*****, 2017, 198: 000–000.**

Approximately 2–3 million years ago (mya), our ancestors inactivated the gene encoding CMP–*N*-acetylneuraminic acid (Neu5Ac) hydroxylase (CMAH), an enzyme that adds a single oxygen atom to the *N*-acetyl group of the sialic acid Neu5Ac, converting it to the hydroxylated form, *N*-glycolylneuraminic acid (Neu5Gc) (1). Because *CMAH* is homozygously pseudogenized in all humans, this mutation resulted in the loss of tens of millions of hydroxyl groups from the plasma membrane surface of most cell types (2). The overall consequences of human *CMAH* loss are being investigated by multiple approaches, including studies of mice harboring a human-like mutation in *Cmah* (3). Studies in such mice indicate that partial reproductive incompatibility due to Neu5Gc loss ∼2–3 mya likely contributed to speciation of the genus *Homo* (4), which also happens to be a time when the risk of injury and novel infections may have also increased due to scavenging and hunting, involving butchery of animal carcasses with stone tools (5–10). We also reported a difference in human and chimpanzee lymphocyte activation (11, 12) and showed that feeding Neu5Gc (which is metabolically incorporated and displayed) to activated human lymphocytes suppresses their proliferative response (13). Additionally, loss of *Cmah* function accelerates the pathological progression of the mdx and LGMD2D mouse models of human muscular dystrophy (14, 15), concomitant with increased CD68^{+} innate immune cell recruitment to muscles and increased muscle production of inflammatory cytokines, including IL-1β and MCP-1.

Tissue injury invokes a complex repair and regenerative response, which is substantially facilitated and potentiated by the resident and recruited host innate immune system (16–22). Classically, the first responders to tissue injury are the resident macrophage population, followed by neutrophils, which are rapidly recruited from circulating blood to the site of injury (23, 24). Blood monocytes are also recruited and produce many inflammatory components (25–27). The next wave of innate immune cell recruitment involves a more

*Glycobiology Research and Training Center, University of California, San Diego, La Jolla, CA 92093; †Department of Medicine, University of California, San Diego, La Jolla, CA 92093; ‡Department of Cellular and Molecular Medicine, University of California, San Diego, La Jolla, CA 92093; §Department of Pediatrics, University of California, San Diego, La Jolla, CA 92093; ¶Skaggs School of Pharmacy and Pharmaceutical Sciences, University of California, San Diego, La Jolla, CA 92093; ‖Initiative for Maximizing Student Development Program, University of California, San Diego, La Jolla, CA 92093; #Department of Pediatrics, The Ohio State University College of Medicine, Columbus, OH 42305; **Department of Physiology and Cell Biology, The Ohio State University College of Medicine, Columbus, OH 43210; and ††Center for Gene Therapy, The Research Institute at Nationwide Children's Hospital, Columbus, OH 43205

ORCIDs: 0000-0002-3705-9060 (J.J.O.); 0000-0003-4344-3592 (C.K.G.); 0000-0002-2206-975X (A.V.).

Received for publication August 24, 2016. Accepted for publication January 4, 2017.

This work was supported by National Institutes of Health Grants R01GM32373 (to A.V.) and R01AR060949 (to P.T.M.), as well as by the Mathers Foundation of New York. Blood samples from chimpanzees were provided by the Yerkes Primate Center (Atlanta, GA) under National Institutes of Health Base Grant ORIP/OD P51OD011132.

Address correspondence and reprint requests to Dr. Ajit Varki, University of California, San Diego, 9500 Gilman Drive, MC 0687, La Jolla, CA 92093-0687. E-mail address: a1varki@ucsd.edu

The online version of this article contains supplemental material.

Abbreviations used in this article: CMAH, CMP–*N*-acetylneuraminic acid hydroxylase; LAP, latency-associated peptide; LB, Luria–Bertani; mya, million years ago; Neu5Ac, *N*-acetylneuraminic acid; Neu5Gc, *N*-glycolylneuraminic acid; RNA-seq, RNA sequencing; WT, wild-type.

complex anti-inflammatory macrophage population (28–30), which facilitates wound healing (31–33). Dysregulation of these inflammatory and anti-inflammatory pathways during chronic disorders can lead to unrestrained inflammation, ultimately leading to an increase in tissue fibrosis and, in some cases, tissue loss (34–37).

TLRs, which are innate pattern recognition receptors, are master regulators of the innate inflammatory status of cells (38, 39). TLRs also recognize and potentiate the first line of host defense against pathogens. Recently, TLR4 has been implicated in the pathology of muscular dystrophy, wherein muscles are in a chronically inflamed state (18). Classically, LPS, which can be released from the outer membrane of Gram-negative bacteria, stimulates the production and secretion of proinflammatory cytokines such as TNF-α, IL-6, and IL-1β (40–44). LPS is recognized by TLR4, which is part of the LPS receptor complex, along with CD14 and MD-2. TLR4 contains nine *N*-linked glycans in its ectodomain, two of which are required for its membrane localization and others that are important for proper LPS binding (45).

Sialic acids such as Neu5Ac and Neu5Gc commonly terminate these N-linked glycan chains, and their density and signaling influence can be affected by the action of endogenous neuraminidase 1 (a sialidase) (46–49). Sialic acid–bearing glycosphingolipids (gangliosides) that densely populate lipid rafts on cell membranes have also been shown to directly influence the translocation of TLR4 into lipid rafts after LPS stimulation (50). The specific impact of human *CMAH*/Neu5Gc loss has not been explored in these systems. Therefore, we focused our investigation on the impact of *Cmah* loss on innate immune responses, as a model for how Neu5Gc loss could have altered inflammatory physiology during evolution of the genus *Homo*.

Materials and Methods

Isolation of monocytes

Chimpanzee blood samples were collected into EDTA-containing tubes during routine noninvasive health screens of chimpanzee subjects at the Yerkes National Primate Center (Emory University, Atlanta, GA) under local Institutional Review Board approval by Emory University. All collections were made under the rules prevailing prior to the September 15, 2015 designation of captive chimpanzees as endangered species (51). Chimpanzee blood samples were shipped overnight on ice to the University of California, San Diego. Human blood was collected at about the same time into identical tubes from healthy volunteer donors (following informed consent, under the approval from the University of California, San Diego Human Subjects Institutional Review Board) and stored overnight on ice to ensure similar treatment conditions prior to analysis. All health and safety issues related to handling of human and nonhuman primate samples are covered by an institutional biosafety approval from the University of California, San Diego Environmental Health and Safety Committee. All individuals who handle the samples received the required training regarding precautions for bloodborne pathogens. PBMCs were separated over Ficoll-Paque Plus (GE Healthcare, Uppsala, Sweden), followed by positive selection for monocytes using a CD14 MACS system (Miltenyi Biotech, Bergisch Gladbach, Germany), according to the manufacturers' protocols.

Intracellular TNF labeling and cytokine release detection

One million monocytes were seeded per well of a 48-well plate or 100,000 macrophages per well in a 24-well plate were stimulated with varying doses of LPS, whereas unstimulated cells served as negative controls. Stimulation for all assays was conducted at 37˚C and 5% CO_2 in the presence of 0.5 mg/ml brefeldin A (Sigma-Aldrich, St. Louis, MO) to inhibit cellular cytokine release. The intracellular cytokine content was determined after 4 h of stimulation. Briefly, cells were fixed and permeabilized using Fix Buffer I and Perm/Wash Buffer I (BD Biosciences, San Jose, CA) and stained for intracellular TNF-α. Samples were analyzed with a FACSCalibur (BD Biosciences). The frequencies of cytokine-positive cells were determined by subsequent analysis using FlowJo software (Tree Star).

Animals

All animal experiments were conducted under approved protocols and according to the regulations and guidelines of the Institutional Animal Care and Use Committee at the University of California, San Diego. Male and female *Cmah*$^{-/-}$ C57BL/6 mice (Harlan Laboratories) 8–10 wk of age were injected with 30 mg/kg LPS (Sigma-Aldrich, L2880, lot no. 044M4004V) and monitored during the period of 72 h for mortality.

Lung infection model

The murine sublethal lung infection model was performed with slight modifications, as previously described (52). *Escherichia coli* cultures were grown overnight in Luria–Bertani (LB) medium at 37˚C with shaking and then regrown in the morning in fresh LB medium to a concentration of OD_{600} of 0.4. Bacteria were washed twice with PBS via centrifugation at 3220 × *g* at room temperature and concentrated in PBS to yield 5×10^6 CFU in 40 μl, the inoculation volume. Mice were anesthetized with 100 mg/kg ketamine and 10 mg/kg xylazine. Once sedated, the vocal chords were visualized using an operating otoscope (Welch Allyn), and 40 μl of bacteria was instilled into the trachea during inspiration using a plastic gel loading pipette tip. Mice were placed on a warmed pad for recovery. Mice were sacrificed with CO_2 for bacterial counts 24 h postinfection. To enumerate total surviving bacteria in the lungs, both lung lobes were removed and placed in a 2 ml of a sterile micro tube (Sarstedt) containing 1 ml of PBS and 1-mm silica beads (Biospec). Lungs were homogenized by shaking twice at 6000 rpm for 1 min using a MagNA Lyser (Roche), with the specimens placed on ice as soon as they were harvested. Aliquots from each tube were serially diluted for CFU enumeration on LB medium plates.

Mouse bone marrow–derived macrophages

BMDMs were isolated from the femurs and tibia of 8- to 12-wk-old wild-type (WT) and *Cmah*$^{-/-}$ C57BL/6 mice. Femurs and tibias were flushed with room temperature DMEM, and precursor cells were cultured in RPMI 1640 containing 20% FBS, 1% penicillin-streptomycin, and 50 ng/ml M-CSF at 37˚C in 5% CO_2 for 7 d, with changes of media on day 4. One day prior to LPS stimulation, cells were lifted with 5 mM EDTA and 300,000 cells per well were seeded in a 24-well plate in RPMI 1640 containing 10% FBS.

Mouse peritoneal macrophages

Peritoneal macrophages from 8- to 12-wk-old WT and *Cmah*$^{-/-}$ C57BL/6 mice were harvested 4 d after 2.5 ml of 3% thioglycolate i.p. injection. A total volume of 10 ml of ice-cold PBS was used to extract 7–8 ml of peritoneal lavage. Cells were separated by adherence overnight, washed with PBS, lifted with 5 mM EDTA, and then 300,000 cells per well in a 24-well plate or 100,000 cells per well in a 96-well plate were seeded in RPMI 1640 containing 10% FBS.

Human and chimpanzee monocyte–derived macrophages

Human or chimpanzee PBMCs isolated from 20 ml of blood were plated in one 24-well plate. Monocytes were separated by overnight adhesion in RPMI 1640 containing 10% FBS and 1% penicillin-streptomycin. Cell culture media were then carefully replaced with RPMI 1640 containing 10% FBS and 100 ng/ml human M-CSF without washing. Cells were allowed to differentiate in the presence of M-CSF for 5 d. Additional RPMI 1640 plus 10% FBS plus 100 ng/ml human M-CSF was added when needed to maintain normal pH. After 5 d, adherent cells were washed twice with PBS and resuspended in the appropriate experimental conditions.

Quantification of sialic acid content by 1,2-diamino-4,5-methylenedioxybenzene–HPLC

Quantification of sialic acid content and type on acid-hydrolyzed samples of vertebrate tissues, polymers, and disaccharides was done using previously described methods of 1,2-diamino-4,5-methylenedioxybenzene derivatization at 50˚C for 2.5 h (53), followed by HPLC fluorometry on a Phenomenex C18 column using an isocratic elution in 85% water, 7% methanol, and 8% acetonitrile.

Macrophage phagocytosis assay

pHrodo Red *E. coli* (Thermo Fisher, P35361) and *Staphylococcus aureus* (Thermo Fisher, A10010) BioParticles conjugates for phagocytosis were used exactly as indicated by the manufacturer's protocol. One hundred thousand peritoneal macrophages per well were incubated with 100 μl of pHrodo BioParticles suspension for 1 or 2 h. For confocal microscopy, cells were fixed in 2% paraformaldehyde/PBS at 4˚C and then imaged by fluorescence microscopy at the exact same exposure.

Macrophage bacterial killing assay

A single *E. coli* K12 colony was inoculated in LB medium and incubated overnight on a shaker at 37˚C. The next day, inoculum was diluted 1:100

and OD was monitored up to 0.4 (corresponding to ~2 × 10^8 CFU/ml). Bacteria were washed once with PBS and resuspended in appropriate cell culture media. Bacteria were then added to plates, centrifuged at 500 × *g* for 10 min, and then incubated with cells at 37°C. Macrophages were then lysed with 0.05% TX-100, scraped with a rubber stopper, and plated. Neutrophils and whole blood were diluted in the same lysis buffer before plating. Inoculum and all other samples were plated at four different dilutions (10^{-1} to 10^{-4}) in triplicates. Percentage survival was calculated as the experimental sample CFU divided by the initial inoculum CFU.

LPS binding assay

Peritoneal lavage from WT and *Cmah*$^{-/-}$ mice was resuspended at 2 million cells/ml in cold PBS and handled on ice. Cell fluorescence was collected in real time by flow cytometry at a rate of ~1000/s for 10 s. The tube was then removed and 10 μg of fluorescent LPS (Sigma-Aldrich, F8666) was added followed by a quick vortex. The tube was then immediately returned to the flow cytometer and measured in real time for an additional 2 min.

RNA sequencing

Total RNA was assessed for quality using an Agilent TapeStation, with RNA integrity numbers ranging from 8.8 to 10.0. RNA libraries were generated using Illumina's TruSeq stranded mRNA sample preparation kit using 100 ng of RNA following the manufacturer's instructions, modifying the shear time to 5 min. RNA libraries were multiplexed and sequenced with 50-bp single-end reads to a depth of ~20 million reads per sample on an Illumina HiSeq 4000.

Statistical analysis

Error data represent SEM of the results. When comparing WT versus *Cmah*$^{-/-}$ or human versus chimpanzee macrophages, statistical analysis was performed using two-way ANOVA followed by the Tukey multiple comparisons test. For Neu5Ac and Neu5Gc feeding experiments on the same cells, a Student paired two-tailed *t* test was performed. For the survival assay, statistical significance was evaluated using the log-rank (Mantel–Cox) test with a 95% confidence interval (GraphPad Prism, version 7.0a). *$p < 0.05$, **$p < 0.01$, and ***$p < 0.001$ represent statistical significance. For RNA sequencing (RNA-seq), *q* values were determined using DESeq2 differential expression analysis.

Results

Mice and macrophages with a human-like loss of Neu5Gc show enhanced sensitivity to LPS activation

To simulate the immediate effects of *CMAH* loss in the human lineage ~2–3 mya, we compared WT and congenic *Cmah*$^{-/-}$ mice (Fig. 1A). First, we determined the impact of Neu5Gc on the LPS response in vivo by injecting WT and *Cmah*$^{-/-}$ mice with potentially lethal doses of LPS and monitoring survival. At multiple doses, *Cmah*$^{-/-}$ mice exhibited a significant reduction in survival rate compared with WT controls (Fig. 1B–D). Next, we assessed the specific role of Neu5Gc in the macrophage inflammatory response by comparing LPS responses of macrophages derived from bone marrow or the peritoneal cavity. After 24 h of stimulation, bone marrow–derived macrophages from *Cmah*$^{-/-}$ mice produced more inflammatory IL-6 (Fig. 1E) and peritoneal macrophages secreted higher levels of MCP-1 (Fig. 1F). Notably, these phenotypes were not due to differential expression of the LPS receptor TLR4 (Supplemental Fig. 1A) or changes in LPS binding (Supplemental Fig. 1B). We concluded that macrophages from *Cmah*$^{-/-}$ mice exhibit higher sensitivity to LPS, possibly due to differences in signaling.

Macrophages from mice with a human-like loss of Neu5Gc show increased phagocytosis and killing of bacteria

We next explored a more functionally relevant benefit of a stronger innate inflammatory response: the ability to clear and kill bacteria. We checked the capability of mouse peritoneal macrophages to kill

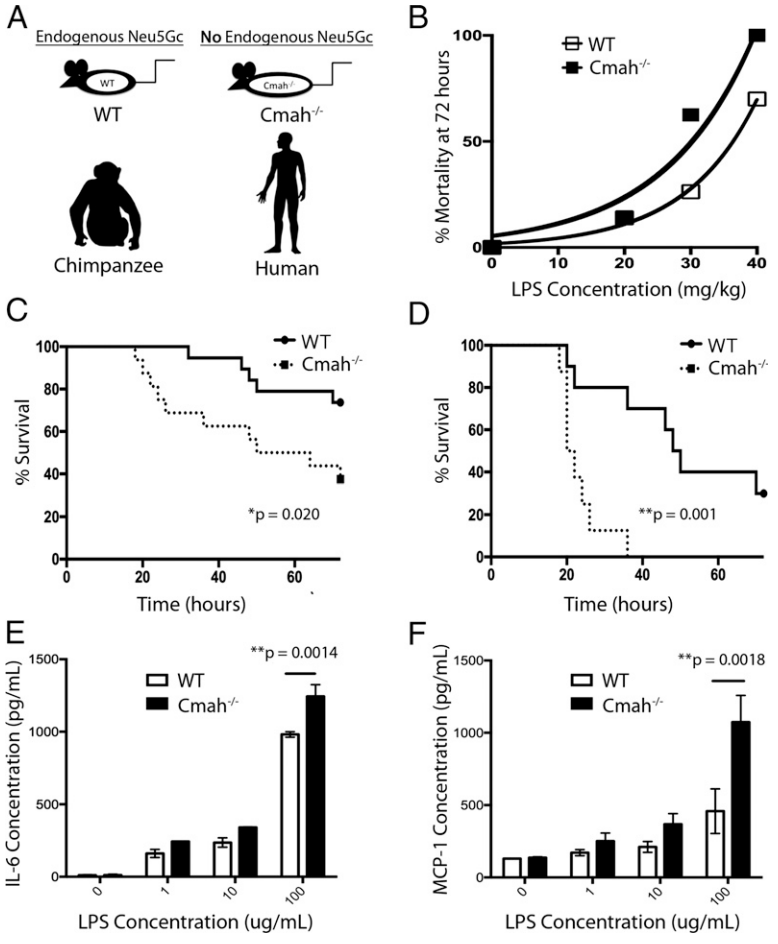

FIGURE 1. Comparison of the inflammatory response and endotoxin binding in WT and *Cmah*$^{-/-}$ mice. (**A**) Humans and *Cmah*$^{-/-}$ mice lack endogenous Neu5Gc, whereas WT mice and chimpanzees have high Neu5Gc expression. (**B**) WT and *Cmah*$^{-/-}$mice were subjected to lethal LPS challenge at different doses (20 mg/kg, $n = 7$; 30 mg/kg, $n = 16$; 40 mg/kg, $n = 8$) and percentage mortality at 72 h was reported for each LPS concentration. (**C**) WT ($n = 19$) and *Cmah*$^{-/-}$ mice ($n = 16$) were subjected to lethal LPS challenge (30 mg/kg). (**D**) WT ($n = 8$) and *Cmah*$^{-/-}$ mice ($n = 10$) were subjected to lethal LPS challenge (40 mg/kg) and survival was monitored for 72 h. (**E**) Bone marrow–derived macrophages ($n = 3$) and (**F**) peritoneal macrophages ($n = 4$) from WT and *Cmah*$^{-/-}$ mice were stimulated for 24 h with LPS and the secreted cytokines in the supernatant were quantified by cytokine bead assay (BD Biosciences).

E. coli and observed a ~50% reduction in recovery of bacteria incubated with *Cmah*$^{-/-}$ macrophages (Fig. 2A). A similar increase in bacterial killing was observed in heparinized whole blood from *Cmah*$^{-/-}$ mice compared with WT controls. (Fig. 2B). To prove that the observed differences were related to the absence of Neu5Gc, we studied peritoneal macrophages isolated from *Cmah*$^{-/-}$ mice that had been fed equal concentrations of either Neu5Ac or Neu5Gc. This approach allows experimental manipulation of cells from the same individual to generate expression of either cell surface Neu5Ac or Neu5Gc, for direct comparison with each other. Free sialic acids in the media can only be taken up through macropinocytosis and used by the cell when they are transported into the cytosol by the endolysosomal transporter sialin (54). Once there, free Neu5Ac or Neu5Gc must be transported to the nucleus to be CMP-activated (55) and then to the Golgi lumen to be conjugated onto glycoproteins or glycolipids. The half-life of free sialic acids fed to cells is ~4 d (56), so most of it should be used in this way after feeding. However, sialic acid degradation to their acetate (from Neu5Ac) and glycolate (from Neu5Gc) metabolites does occur during the constant recycling of endogenous Neu5Ac or Neu5Gc sialic acids during maintenance of steady-state (56–59). Similar to results observed between WT and *Cmah*$^{-/-}$ mice, the feeding of Neu5Gc to peritoneal macrophages isolated from *Cmah*$^{-/-}$ mice indeed increased their Neu5Gc content (Supplemental Fig. 3A) and suppressed their capability to kill bacteria (Fig. 2C).

To determine the effect of *Cmah* loss on bacterial killing in vivo, we infected the lungs of WT and *Cmah*$^{-/-}$ mice with *E. coli* K12 bacteria via intranasal inoculation. At 24 h, *Cmah*$^{-/-}$ mice exhibited a greater capability to clear *E. coli* K12 from the lungs in vivo compared with WT controls (Fig. 2D). WT and *Cmah*$^{-/-}$ peritoneal macrophages were also incubated with *S. aureus* BioParticles that fluoresce when internalized into phagosomes, and we observed a 10-fold increase in macrophage phagocytosis of the fluorescent bacterial particles in *Cmah*$^{-/-}$ macrophages (Fig. 2E, 2F). Taken together, these data suggest that loss of Neu5Gc leads to increased phagocytic activity and bacterial clearance during infection.

Human innate immune cells show increased phagocytosis and killing of bacteria relative to chimpanzees, which is suppressed by Neu5Gc feeding

Chimpanzees have intact CMAH function and express high levels of Neu5Gc on their cell surfaces (60). However, they have diverged independently for ~6–7 mya since the common ancestor with humans, and they also have a significantly higher genetic diversity. The availability of samples was limited to chimpanzees in captivity undergoing routine blood testing during annual health checks (prior to the September 15, 2015 restriction on such ethically reasonable studies) (51). We noted an unexplained technical pitfall associated with positively enriching for chimpanzee CD14^{+} PBMCs, because (unlike human samples) they are commonly contaminated with ~70% neutrophils. Therefore, we compared innate inflammatory response of limited samples of chimpanzee monocytes to those of humans and conducted the rest of our limited comparisons with monocyte-derived macrophages. Monocyte-derived macrophages from humans incubated with *E. coli* exhibited a greater killing capacity compared with chimpanzee controls (Fig. 3A). A similar difference in bacterial killing was

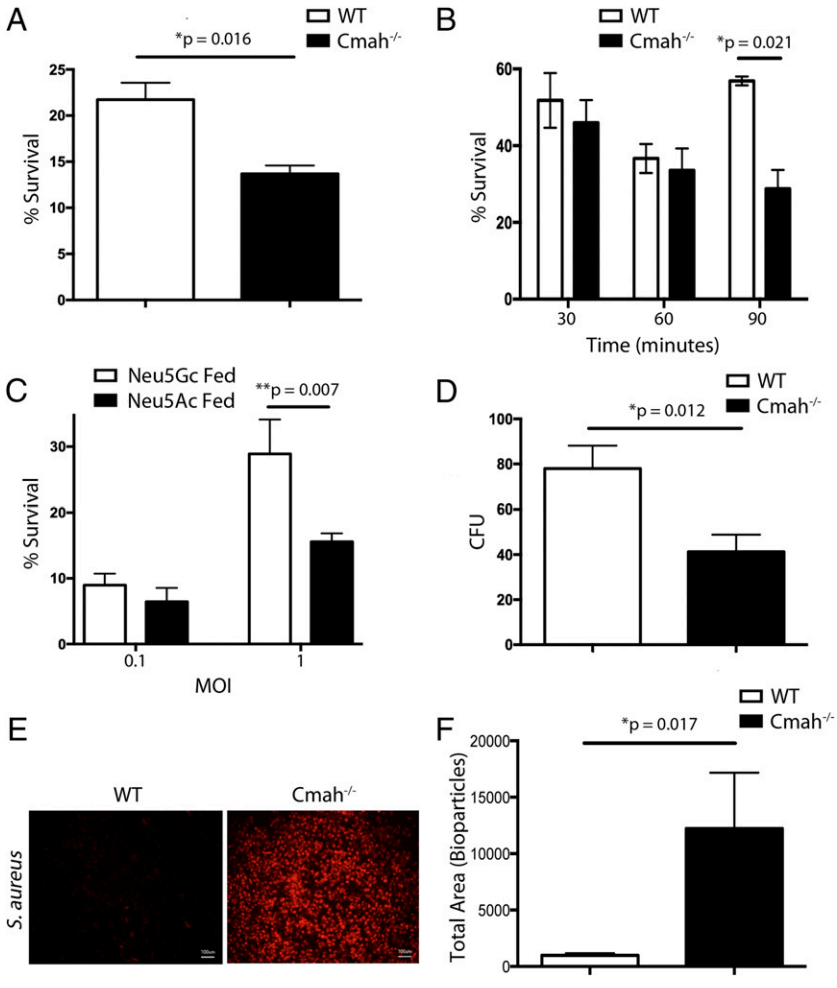

FIGURE 2. Comparison of bacterial killing and phagocytosis in WT and *Cmah*$^{-/-}$ ex vivo and in vivo. (**A**) Peritoneal macrophages from WT and *Cmah*$^{-/-}$ mice were stimulated with *E. coli* K12 for 1 h at a multiplicity of infection (MOI) of 1. (**B**) Whole blood from WT and *Cmah*$^{-/-}$ mice (n = 3) was stimulated with ~4 × 10^{5} CFU of *E. coli* K12 and aliquots were plated at 30, 60, and 90 min. (**C**) Peritoneal macrophages (n = 4) from *Cmah*$^{-/-}$ mice were fed Neu5Ac or Neu5Gc for 4 d, followed by stimulation with *E. coli* K12 for 1 h at MOIs of 0.1 and 1. (**D**) The lungs of WT (n = 9) and *Cmah*$^{-/-}$ (n = 8) mice were infected with 5 × 10^{6} CFU of *E. coli* K12, and bacterial survival was assessed by plating an aliquot of the total lung homogenate 24 h postinfection. (**E**) Peritoneal macrophages from WT and *Cmah*$^{-/-}$ mice were stimulated with pHrodo Red *S. aureus* BioParticles for 2 h. Scale bars, 100 μm. (**F**) Fluorescence of BioParticles from WT and *Cmah*$^{-/-}$ mice was quantified by ImageJ (n = 3).

observed in whole blood from chimpanzees and humans inoculated with *E. coli* (K12) bacteria (Fig. 3B). Similar to *Cmah*$^{-/-}$ mouse macrophages, feeding human monocytes with Neu5Gc substantially reduced their capacity of killing bacteria (Fig. 3C). We tested the same human and chimpanzee monocyte-derived macrophages for both the intracellular TNF-α expression after LPS stimulation and the phagocytosis of *E. coli* or *S. aureus* BioParticles. Macrophages were incubated with LPS in the presence of brefeldin A for 4 h or with the BioParticles for 1 h in the presence of autologous heat-denatured serum. Although we did not observe a statistically significant difference in intracellular TNF-α (Fig. 3D), the same human cells exhibited substantially greater phagocytosis of both *E. coli* and *S. aureus* BioParticles compared with chimpanzee cells (Fig. 3E, 3F).

Peripheral blood monocytes were stimulated with LPS for 4 h and intracellular TNF-α production was measured by flow cytometry. The percentage of TNF-α$^+$ cells was also measured by quantifying intracellular TNF-α levels above baseline levels. Human CD14$^+$ monocytes showed a marginal increase in TNF-α production compared with chimpanzees ex vivo, but this difference was not statistically significant (Supplemental Fig. 2). Considerable variation was also seen, as expected for the individuals from outbred species with varying genetic backgrounds and environmental conditions.

We next differentiated human monocytes into macrophages while feeding the same cells either Neu5Ac or Neu5Gc for 4 d. We observed a significant effect on intracellular TNF-α expression (Fig. 4A, 4B) and *E. coli* BioParticles phagocytosis (Fig. 4C, 4D) in Neu5Gc-fed macrophages compared with Neu5Ac-fed macrophages.

Neu5Gc containing mouse macrophages show differential expression of C/EBPβ

To determine whether Neu5Ac or Neu5Gc feeding differentially altered gene expression, we performed RNA-seq on macrophages from *Cmah*$^{-/-}$ mice that had been fed either Neu5Ac or Neu5Gc for 3 d (Fig. 5A). Although several of the 36 genes that showed significant differential expression (Supplemental Table I) could be affecting macrophage function, C/EBPβ (Fig. 5B) was of major interest because of its role in macrophage development and bacterial killing (61, 62). Therefore, we examined the protein expression of latency-associated peptide (LAP; a 34-kDa C/EBPβ isoform that is transcriptionally active in macrophages) and found that LAP expression is elevated in *Cmah*$^{-/-}$ peritoneal macrophages compared with WT controls (Fig. 5C, 5D).

Discussion

We have suggested that initial hominin loss of *CMAH* may have been selected by an infectious agent, such as the malarial sporozoite recognition of erythrocyte sialic acids (60), and was then fixed relatively rapidly in a new population by virtue of cryptic female choice, mediated by intrauterine anti-Neu5Gc Abs, selecting against ancestral Neu5Gc-positive sperm and/or embryos (4). In this study, we present data suggesting that fixation of the *CMAH*-null state may have then been beneficial for the transition of these hominins toward increased tool usage, butchery of carcasses,

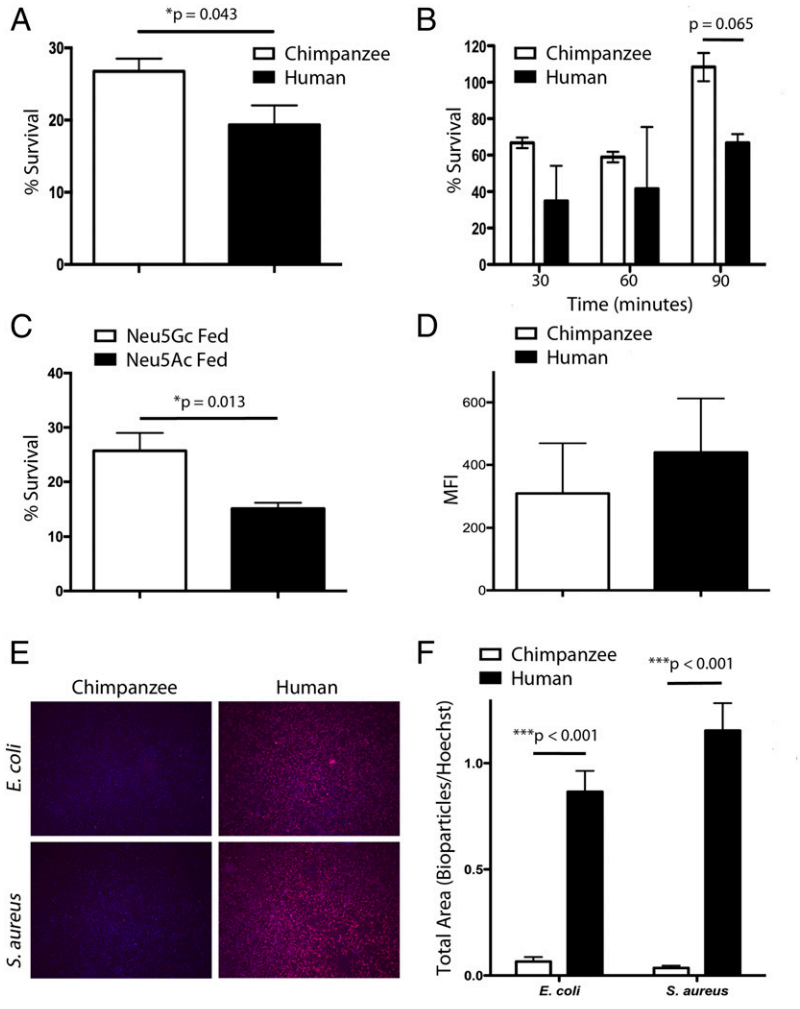

FIGURE 3. Comparison of bacterial killing and phagocytosis in humans and chimpanzees. (**A**) Monocyte-derived macrophages from humans and chimpanzees (n = 6) were stimulated with *E. coli* K12 for 1 h at a multiplicity of infection of 1. (**B**) Whole blood from humans and chimpanzees (n = 2) was stimulated with ~4 × 10^5 CFU of *E. coli* K12 and aliquots were plated at 30, 60, and 90 min. (**C**) Monocyte-derived macrophages from humans (n = 7) were fed 2 mM Neu5Ac or Neu5Gc for 4 d, followed by stimulation with *E. coli* K12 for 1 h at a multiplicity of infection of 1. (**D**) Monocyte-derived macrophages from five humans and four chimpanzees were stimulated with 1 ng/ml LPS for 4 h in the presence of brefeldin A, and intracellular TNF-α expression was quantified by flow cytometry. (**E**) Monocyte-derived macrophages from humans and chimpanzees were stimulated with pHrodo Red *E. coli* or *S. aureus* BioParticles in pooled heat-denatured autologous serum for 1 h and imaged using Keyence BZ-9000 (original magnification ×40). (**F**) Fluorescence of BioParticles from five humans and four chimpanzees was quantified by ImageJ.

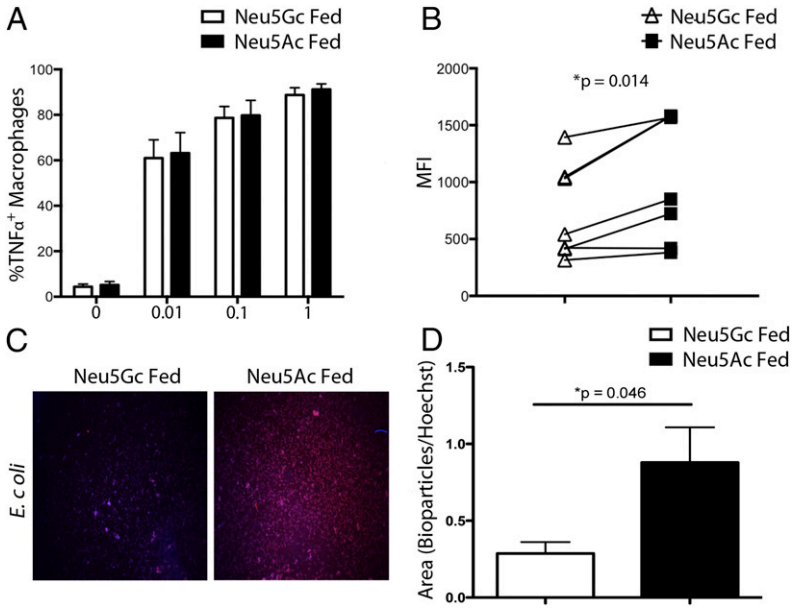

FIGURE 4. Comparison of TNF-α production and phagocytosis in Neu5Gc- and Neu5Ac-fed human macrophages. (**A**) Monocyte-derived macrophages from humans ($n = 7$) were fed 2 mM Neu5Ac or Neu5Gc for 4 d, followed by stimulation with 0–1 ng/ml LPS in the presence of brefeldin A for 4 h and intracellular TNF-α expression was quantified by flow cytometry. (**B**) At one concentration (1 ng/ml), the effect of Neu5Gc feeding was significant. (**C**) Monocyte-derived macrophages were incubated with pHrodo Red *S. aureus* BioParticles in serum-free conditions for 2 h and imaged using Keyence BZ-9000 (original magnification ×40). (**D**) Fluorescence of BioParticles from four individuals fed either Neu5Ac or Neu5Gc was quantified by ImageJ.

and exposure to novel pathogens. Approximately 2–3 mya, when *CMAH* loss is likely to have been fixed in our lineage (1), the fossils of late *Australopithecus* and early *Homo* are found surrounded by Oldowan stone tools, presumably used to break bones and eat nutrient-rich bone marrow (5, 6, 8, 63). This activity likely resulted in superficial injuries, combined with exposure to new bacterial pathogens, potentially leading to a greater prevalence of infection.

Under these novel circumstances, the ability to kill and clear sublethal doses of bacteria at a greater capacity could have been beneficial for the utilization of stone tools and the consumption of other animals. Alternatively, just as other ancestral mutations have become deleterious for specific modern pathologies (64, 65), *CMAH* loss may be a deleterious contributor to endotoxemia in humans today who experience overwhelming infections and sepsis (66).

Understanding the immediate effect of *CMAH* loss on ancient hominin physiology is impossible. Our best efforts are to compare humans versus chimpanzees ex vivo and *Cmah*$^{-/-}$ versus WT mice ex vivo and in vivo. When comparing humans and chimpanzee macrophages ex vivo, we see a nonsignificant difference in inflammatory responses in the same conditions where we see significant differences in bacterial killing and phagocytosis. When studying the immediate effects of *Cmah* loss in mice, we see similar results: profound effects on bacterial killing, yet a relatively mild inflammatory phenotype ex vivo. Importantly, our experimental evidence also illustrates an increased sensitivity of *Cmah*$^{-/-}$ mice to endotoxic shock in vivo, which could be due to multiple mechanisms and other cell types. More work is needed to determine whether an altered innate immune response in *Cmah*$^{-/-}$ mice contributes to other observed phenotypes, such as delayed wound healing (3), greater inflammation and fibrosis in the mdx model of muscular dystrophy (14), and increased growth of transplanted human tumor cells (67). We speculate that these and other human chronic inflammatory states could be modeled in *Cmah*$^{-/-}$ mice.

Fully explaining all mechanisms underlying these phenotypic differences is complex and difficult. Given the global impact of eliminating tens of millions of *N*-glycolyl groups from cells via

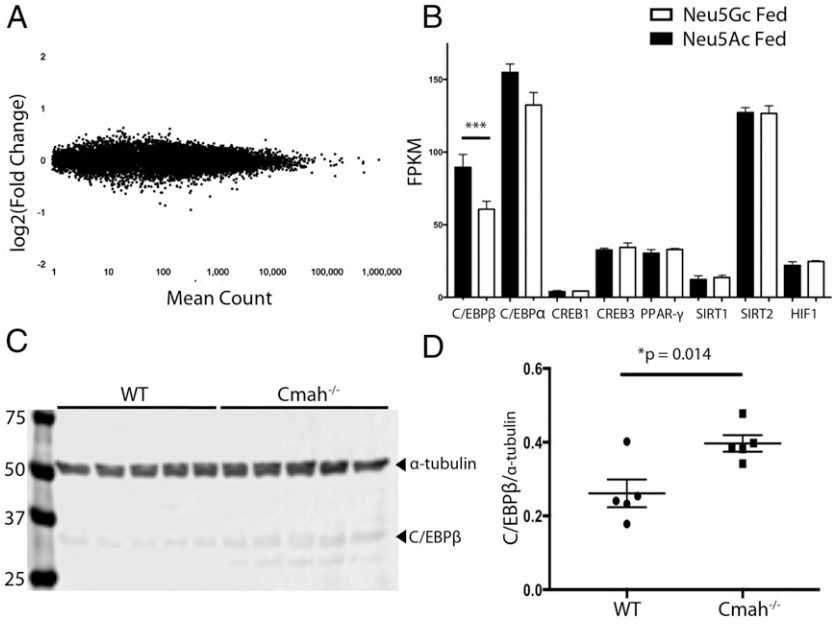

FIGURE 5. C/EBPβ expression is suppressed by the presence of Neu5Gc. (**A**) MA plot of total RNA-seq results, comparing peritoneal macrophages isolated from *Cmah*$^{-/-}$ mice ($n = 3$) fed either 2 mM Neu5Ac or 2 mM Neu5Gc for 3 d. (**B**) C/EBPβ expression was suppressed in macrophages that had been fed Neu5Gc (***$q = 0.000495$ by DESeq analysis). (**C**) Peritoneal macrophages from WT and *Cmah*$^{-/-}$ mice ($n = 5$) were immunoblotted against α-tubulin and LAP, a 34-kDa isoform of C/EBPβ (background was subtracted in ImageJ with rolling ball radius of 100 pixels). (**D**) ImageJ quantification and analysis of WT versus *Cmah*$^{-/-}$ LAP expression levels normalized to α-tubulin levels.

CMAH loss, there are multiple possible (and mutually nonexclusive) mechanisms contributing to our findings. For example, cytosolic degradation of excess Neu5Gc can result in generation of glycolate (instead of acetate generated from Neu5Ac breakdown) (56), with the possibility of a systematic alteration in cell metabolism. Previously published microarray data in WT and *Cmah*$^{-/-}$ mouse muscle implicated CREB1, C/EBPα, and C/EBPβ as candidate transcription factors affected by *Cmah* loss (14). Alterations in these transcription factors have been shown to affect both macrophage activation and systemic metabolism (61, 68–70) and appear to be differentially expressed and regulated in different tissue types of WT versus *Cmah*$^{-/-}$ mice. C/EBPβ expression is also suppressed in macrophages fed Neu5Gc and C/EBPβ (NF-IL6) knockout mice are known to experience a drastic reduction in the capability of their monocytes to kill bacteria (62, 70, 71).

It is also possible that Neu5Gc loss altered cell surface neuraminidase activity. Multiple reports have implicated neuraminidase 1 as an important regulator of the TLR4 response (47), and we previously reported that neuraminidase 1 prefers Neu5Ac to Neu5Gc in the α2–8 linkages common in polysialic acids (72). The endogenous neuraminidase preference for α2–3- or α2–6-linked Neu5Ac and Neu5Gc, which are common on the surface of innate immune cells, needs further study. A further non–mutually exclusive possibility is that the loss of millions of hydrophilic cell surface hydroxyl groups on Neu5Gc (replaced by hydrophobic acetyl groups on Neu5Ac) led to global changes in cell surface biophysics, which could have global ramifications on cell surface receptor localization, clustering, and signaling. It is reasonable to hypothesize that the cell membranes of humans and *Cmah*$^{-/-}$ mice are overall more hydrophobic than chimpanzee or WT counterparts. Further investigations are needed to determine whether global changes in cell surface biophysics occur after *Cmah* loss.

Due to a limitation in the amount of samples combined with a high genetic variation, it is also difficult to study the differences in inflammatory physiology between humans and chimpanzees. Our results are consistent with previous studies that have established that humans and chimpanzees respond at the same order of magnitude to endotoxin (43, 73–76). However, direct comparisons of humans and chimpanzees with the same batch of LPS at multiple doses in vivo is no longer possible, nor is it possible to compare survival after endotoxic shock between humans and chimpanzees with the same batch and dose of endotoxin. Limited evidence using different batches of *E. coli* endotoxin could suggest a difference between humans and chimpanzees, but they are not directly comparable. For example, peak serum TNF-α (68–1374 pg/ml) and IL-6 (72–2820 pg/ml) secretion of humans in response to 2 ng/kg *E. coli* endotoxin bolus injection (74) is more sensitive than the serum TNF-α (188 ± 54 pg/ml) and IL-6 (138 ± 37 pg/ml) concentrations of chimpanzees in response to 4 ng/kg *E. coli* endotoxin bolus injection (73). Regardless, when we compared human and chimpanzee macrophages ex vivo, we did not observe a statistically significant difference in the inflammatory response to LPS in exactly the same conditions where we did observe a difference in both bacterial killing and phagocytosis of BioParticles.

Furthermore, millions of years have passed since humans and chimpanzees diverged from each other (77, 78). Therefore, studying differences in *Cmah*$^{-/-}$ and WT mice allows for greater sample sizes with much less genetic variation. Overall, we observed similar results in *Cmah*$^{-/-}$ versus WT mice as we did in humans versus chimpanzees, and *Cmah*$^{-/-}$ mice are useful as a model for human evolution as well as human disease susceptibility.

Although much further work is needed to define the multiple consequences of *CMAH*/Neu5Gc loss during human evolution, our current work suggests that there were likely complex effects on innate immunity, apparently providing a greater capability to clear sublethal bacterial challenges, possibly at the cost of increased risk of endotoxic shock. These findings may also help explain why the *Cmah*-null state alters disease severity in mouse models of human disease associated with inflammation, such as muscular dystrophy. They are also relevant to future modeling of human infectious disease states in mice.

Acknowledgments

We thank Yuko Naito-Matsui, Anel Lizcano, and Shoib Siddiqui for help in the laboratory. RNA-seq was conducted at the Institute for Genomic Medicine Genomics Center, University of California, San Diego, La Jolla, CA.

Disclosures

The authors have no financial conflicts of interest.

References

1. Chou, H. H., H. Takematsu, S. Diaz, J. Iber, E. Nickerson, K. L. Wright, E. A. Muchmore, D. L. Nelson, S. T. Warren, and A. Varki. 1998. A mutation in human CMP-sialic acid hydroxylase occurred after the *Homo-Pan* divergence. *Proc. Natl. Acad. Sci. USA* 95: 11751–11756.
2. Varki, A., and P. Gagneux. 2012. Multifarious roles of sialic acids in immunity. *Ann. N. Y. Acad. Sci.* 1253: 16–36.
3. Hedlund, M., P. Tangvoranuntakul, H. Takematsu, J. M. Long, G. D. Housley, Y. Kozutsumi, A. Suzuki, A. Wynshaw-Boris, A. F. Ryan, R. L. Gallo, et al. 2007. *N*-glycolylneuraminic acid deficiency in mice: implications for human biology and evolution. *Mol. Cell. Biol.* 27: 4340–4346.
4. Ghaderi, D., S. A. Springer, F. Ma, M. Cohen, P. Secrest, R. E. Taylor, A. Varki, and P. Gagneux. 2011. Sexual selection by female immunity against paternal antigens can fix loss of function alleles. *Proc. Natl. Acad. Sci. USA* 108: 17743–17748.
5. Semaw, S., P. Renne, J. W. Harris, C. S. Feibel, R. L. Bernor, N. Fesseha, and K. Mowbray. 1997. 2.5-Million-year-old stone tools from Gona, Ethiopia. *Nature* 385: 333–336.
6. Baird, A., T. Costantini, R. Coimbra, and B. P. Eliceiri. 2016. Injury, inflammation and the emergence of human-specific genes. *Wound Repair Regen.* 24: 602–606.
7. McPherron, S. P., Z. Alemseged, C. W. Marean, J. G. Wynn, D. Reed, D. Geraads, R. Bobe, and H. A. Béarat. 2010. Evidence for stone-tool-assisted consumption of animal tissues before 3.39 million years ago at Dikika, Ethiopia. *Nature* 466: 857–860.
8. Harmand, S., J. E. Lewis, C. S. Feibel, C. J. Lepre, S. Prat, A. Lenoble, X. Boës, R. L. Quinn, M. Brenet, A. Arroyo, et al. 2015. 3.3-Million-year-old stone tools from Lomekwi 3, West Turkana, Kenya. *Nature* 521: 310–315.
9. Sayers, K., and C. O. Lovejoy. 2014. Blood, bulbs, and bunodonts: on evolutionary ecology and the diets of *Ardipithecus*, *Australopithecus*, and early *Homo*. *Q. Rev. Biol.* 89: 319–357.
10. O'Connell, J. F., K. Hawkes, K. D. Lupo, and N. G. Blurton Jones. 2002. Male strategies and Plio-Pleistocene archaeology. *J. Hum. Evol.* 43: 831–872.
11. Soto, P. C., L. L. Stein, N. Hurtado-Ziola, S. M. Hedrick, and A. Varki. 2010. Relative over-reactivity of human versus chimpanzee lymphocytes: implications for the human diseases associated with immune activation. *J. Immunol.* 184: 4185–4195.
12. Soto, P. C., M. Y. Karris, C. A. Spina, D. D. Richman, and A. Varki. 2013. Cell-intrinsic mechanism involving Siglec-5 associated with divergent outcomes of HIV-1 infection in human and chimpanzee CD4 T cells. *J. Mol. Med. (Berl.)* 91: 261–270.
13. Buchlis, G., P. Odorizzi, P. C. Soto, O. M. Pearce, D. J. Hui, M. S. Jordan, A. Varki, E. J. Wherry, and K. A. High. 2013. Enhanced T cell function in a mouse model of human glycosylation. *J. Immunol.* 191: 228–237.
14. Chandrasekharan, K., J. H. Yoon, Y. Xu, S. deVries, M. Camboni, P. M. Janssen, A. Varki, and P. T. Martin. 2010. A human-specific deletion in mouse *Cmah* increases disease severity in the mdx model of Duchenne muscular dystrophy. *Sci. Transl. Med.* 2: 42ra54.
15. Martin, P. T., M. Camboni, R. Xu, B. Golden, K. Chandrasekharan, C. M. Wang, A. Varki, and P. M. Janssen. 2013. *N*-Glycolylneuraminic acid deficiency worsens cardiac and skeletal muscle pathophysiology in α-sarcoglycan-deficient mice. *Glycobiology* 23: 833–843.
16. Gurtner, G. C., S. Werner, Y. Barrandon, and M. T. Longaker. 2008. Wound repair and regeneration. *Nature* 453: 314–321.
17. Koh, T. J., and L. A. DiPietro. 2011. Inflammation and wound healing: the role of the macrophage. *Expert Rev. Mol. Med.* 13: e23.
18. Giordano, C., K. Mojumdar, F. Liang, C. Lemaire, T. Li, J. Richardson, M. Divangahi, S. Qureshi, and B. J. Petrof. 2015. Toll-like receptor 4 ablation in mdx mice reveals innate immunity as a therapeutic target in Duchenne muscular dystrophy. *Hum. Mol. Genet.* 24: 2147–2162.
19. Brinkworth, J. F., and L. B. Barreiro. 2014. The contribution of natural selection to present-day susceptibility to chronic inflammatory and autoimmune disease. *Curr. Opin. Immunol.* 31: 66–78.

20. De Maio, A., M. B. Torres, and R. H. Reeves. 2005. Genetic determinants influencing the response to injury, inflammation, and sepsis. *Shock* 23: 11–17.
21. Medzhitov, R. 2008. Origin and physiological roles of inflammation. *Nature* 454: 428–435.
22. Tabas, I., and C. K. Glass. 2013. Anti-inflammatory therapy in chronic disease: challenges and opportunities. *Science* 339: 166–172.
23. Klebanoff, S. J., A. J. Kettle, H. Rosen, C. C. Winterbourn, and W. M. Nauseef. 2013. Myeloperoxidase: a front-line defender against phagocytosed microorganisms. *J. Leukoc. Biol.* 93: 185–198.
24. Kim, N. D., and A. D. Luster. 2015. The role of tissue resident cells in neutrophil recruitment. *Trends Immunol.* 36: 547–555.
25. Németh, T., and A. Mócsai. 2016. Feedback amplification of neutrophil function. *Trends Immunol.* 37: 412–424.
26. Mogensen, T. H. 2009. Pathogen recognition and inflammatory signaling in innate immune defenses. *Clin. Microbiol. Rev.* 22: 240–273, Table of Contents.
27. Aderem, A. 2003. Phagocytosis and the inflammatory response. *J. Infect. Dis.* 187(Suppl. 2): S340–S345.
28. Soehnlein, O., and L. Lindbom. 2010. Phagocyte partnership during the onset and resolution of inflammation. *Nat. Rev. Immunol.* 10: 427–439.
29. Varin, A., S. Mukhopadhyay, G. Herbein, and S. Gordon. 2010. Alternative activation of macrophages by IL-4 impairs phagocytosis of pathogens but potentiates microbial-induced signalling and cytokine secretion. *Blood* 115: 353–362.
30. Okabe, Y., and R. Medzhitov. 2016. Tissue biology perspective on macrophages. *Nat. Immunol.* 17: 9–17.
31. Deng, B., M. Wehling-Henricks, S. A. Villalta, Y. Wang, and J. G. Tidball. 2012. IL-10 triggers changes in macrophage phenotype that promote muscle growth and regeneration. *J. Immunol.* 189: 3669–3680.
32. Kharraz, Y., J. Guerra, C. J. Mann, A. L. Serrano, and P. Muñoz-Cánoves. 2013. Macrophage plasticity and the role of inflammation in skeletal muscle repair. *Mediators Inflamm.* 2013: 491497.
33. Burzyn, D., W. Kuswanto, D. Kolodin, J. L. Shadrach, M. Cerletti, Y. Jang, E. Sefik, T. G. Tan, A. J. Wagers, C. Benoist, and D. Mathis. 2013. A special population of regulatory T cells potentiates muscle repair. *Cell* 155: 1282–1295.
34. Mann, C. J., E. Perdiguero, Y. Kharraz, S. Aguilar, P. Pessina, A. L. Serrano, and P. Muñoz-Cánoves. 2011. Aberrant repair and fibrosis development in skeletal muscle. *Skelet. Muscle* 1: 21.
35. Lieber, R. L., and S. R. Ward. 2013. Cellular mechanisms of tissue fibrosis. 4. Structural and functional consequences of skeletal muscle fibrosis. *Am. J. Physiol. Cell Physiol.* 305: C241–C252.
36. Chovatiya, R., and R. Medzhitov. 2014. Stress, inflammation, and defense of homeostasis. *Mol. Cell* 54: 281–288.
37. Nathan, C., and A. Ding. 2010. Nonresolving inflammation. *Cell* 140: 871–882.
38. Kanzler, H., F. J. Barrat, E. M. Hessel, and R. L. Coffman. 2007. Therapeutic targeting of innate immunity with Toll-like receptor agonists and antagonists. *Nat. Med.* 13: 552–559.
39. Moresco, E. M., D. LaVine, and B. Beutler. 2011. Toll-like receptors. *Curr. Biol.* 21: R488–R493.
40. Lu, Y. C., W. C. Yeh, and P. S. Ohashi. 2008. LPS/TLR4 signal transduction pathway. *Cytokine* 42: 145–151.
41. Covert, M. W., T. H. Leung, J. E. Gaston, and D. Baltimore. 2005. Achieving stability of lipopolysaccharide-induced NF-κB activation. *Science* 309: 1854–1857.
42. Lawrence, T., M. Bebien, G. Y. Liu, V. Nizet, and M. Karin. 2005. IKKα limits macrophage NF-κB activation and contributes to the resolution of inflammation. *Nature* 434: 1138–1143.
43. Brinkworth, J. F., E. A. Pechenkina, J. Silver, and S. M. Goyert. 2012. Innate immune responses to TLR2 and TLR4 agonists differ between baboons, chimpanzees and humans. *J. Med. Primatol.* 41: 388–393.
44. Warren, H. S., C. Fitting, E. Hoff, M. Adib-Conquy, L. Beasley-Topliffe, B. Tesini, X. Liang, C. Valentine, J. Hellman, D. Hayden, and J. M. Cavaillon. 2010. Resilience to bacterial infection: difference between species could be due to proteins in serum. *J. Infect. Dis.* 201: 223–232.
45. da Silva Correia, J., and R. J. Ulevitch. 2002. MD-2 and TLR4 *N*-linked glycosylations are important for a functional lipopolysaccharide receptor. *J. Biol. Chem.* 277: 1845–1854.
46. Pshezhetsky, A. V., and L. I. Ashmarina. 2013. Desialylation of surface receptors as a new dimension in cell signaling. *Biochemistry (Mosc.)* 78: 736–745.
47. Pshezhetsky, A. V., and A. Hinek. 2011. Where catabolism meets signalling: neuraminidase 1 as a modulator of cell receptors. *Glycoconj. J.* 28: 441–452.
48. Abdulkhalek, S., S. R. Amith, S. L. Franchuk, P. Jayanth, M. Guo, T. Finlay, A. Gilmour, C. Guzzo, K. Gee, R. Beyaert, and M. R. Szewczuk. 2011. Neu1 sialidase and matrix metalloproteinase-9 cross-talk is essential for Toll-like receptor activation and cellular signaling. *J. Biol. Chem.* 286: 36532–36549.
49. Chen, G. Y., N. K. Brown, W. Wu, Z. Khedri, H. Yu, X. Chen, D. van de Vlekkert, A. D'Azzo, P. Zheng, and Y. Liu. 2014. Broad and direct interaction between TLR and Siglec families of pattern recognition receptors and its regulation by Neu1. *eLife* 3: e04066.
50. Nikolaeva, S., L. Bayunova, T. Sokolova, Y. Vlasova, V. Bachteeva, N. Avrova, and R. Parnova. 2015. GM1 and GD1a gangliosides modulate toxic and inflammatory effects of *E. coli* lipopolysaccharide by preventing TLR4 translocation into lipid rafts. *Biochim. Biophys. Acta* 1851: 239–247.
51. Grimm, D. 2015. Animal Welfare. New rules may end U.S. chimpanzee research. *Science* 349: 777.
52. Revelli, D. A., J. A. Boylan, and F. C. Gherardini. 2012. A non-invasive intratracheal inoculation method for the study of pulmonary melioidosis. *Front. Cell. Infect. Microbiol.* 2: 164.
53. Manzi, A. E., S. Diaz, and A. Varki. 1990. High-pressure liquid chromatography of sialic acids on a pellicular resin anion-exchange column with pulsed amperometric detection: a comparison with six other systems. *Anal. Biochem.* 188: 20–32.
54. Bardor, M., D. H. Nguyen, S. Diaz, and A. Varki. 2005. Mechanism of uptake and incorporation of the non-human sialic acid *N*-glycolylneuraminic acid into human cells. *J. Biol. Chem.* 280: 4228–4237.
55. Kean, E. L., A. K. Münster-Kühnel, and R. Gerardy-Schahn. 2004. CMP-sialic acid synthetase of the nucleus. *Biochim. Biophys. Acta* 1673: 56–65.
56. Bergfeld, A. K., O. M. Pearce, S. L. Diaz, T. Pham, and A. Varki. 2012. Metabolism of vertebrate amino sugars with *N*-glycolyl groups: elucidating the intracellular fate of the non-human sialic acid *N*-glycolylneuraminic acid. *J. Biol. Chem.* 287: 28865–28881.
57. Margolis, R. K., and R. U. Margolis. 1973. The turnover of hexosamine and sialic acid in glycoproteins and mucopolysaccharides of brain. *Biochim. Biophys. Acta* 304: 413–420.
58. Ledeen, R. W., J. A. Skrivanek, L. J. Tirri, R. K. Margolis, and R. U. Margolis. 1976. Gangliosides of the neuron: localization and origin. *Adv. Exp. Med. Biol.* 71: 83–103.
59. Ferwerda, W., C. M. Blok, and J. Heijlman. 1981. Turnover of free sialic acid, CMP-sialic acid, and bound sialic acid in rat brain. *J. Neurochem.* 36: 1492–1499.
60. Martin, M. J., J. C. Rayner, P. Gagneux, J. W. Barnwell, and A. Varki. 2005. Evolution of human-chimpanzee differences in malaria susceptibility: relationship to human genetic loss of *N*-glycolylneuraminic acid. [Published erratum appears in 2006 *Proc. Natl. Acad. Sci. USA* 103: 9745.] *Proc. Natl. Acad. Sci. USA* 102: 12819–12824.
61. Huber, R., D. Pietsch, T. Panterodt, and K. Brand. 2012. Regulation of C/EBPβ and resulting functions in cells of the monocytic lineage. *Cell. Signal.* 24: 1287–1296.
62. Tanaka, T., S. Akira, K. Yoshida, M. Umemoto, Y. Yoneda, N. Shirafuji, H. Fujiwara, S. Suematsu, N. Yoshida, and T. Kishimoto. 1995. Targeted disruption of the NF-IL6 gene discloses its essential role in bacteria killing and tumor cytotoxicity by macrophages. *Cell* 80: 353–361.
63. Plummer, T. 2004. Flaked stones and old bones: biological and cultural evolution at the dawn of technology. *Am. J. Phys. Anthropol.* 125(Suppl. 39): 118–164.
64. Raichlen, D. A., and G. E. Alexander. 2014. Exercise, APOE genotype, and the evolution of the human lifespan. *Trends Neurosci.* 37: 247–255.
65. Schwarz, F., S. A. Springer, T. K. Altheide, N. M. Varki, P. Gagneux, and A. Varki. 2016. Human-specific derived alleles of CD33 and other genes protect against postreproductive cognitive decline. *Proc. Natl. Acad. Sci. USA* 113: 74–79.
66. Deutschman, C. S., and K. J. Tracey. 2014. Sepsis: current dogma and new perspectives. *Immunity* 40: 463–475.
67. Hedlund, M., V. Padler-Karavani, N. M. Varki, and A. Varki. 2008. Evidence for a human-specific mechanism for diet and antibody-mediated inflammation in carcinoma progression. *Proc. Natl. Acad. Sci. USA* 105: 18936–18941.
68. Ruffell, D., F. Mourkioti, A. Gambardella, P. Kirstetter, R. G. Lopez, N. Rosenthal, and C. Nerlov. 2009. A CREB-C/EBPβ cascade induces M2 macrophage-specific gene expression and promotes muscle injury repair. *Proc. Natl. Acad. Sci. USA* 106: 17475–17480.
69. Lee, B., L. Qiao, M. Lu, H. S. Yoo, W. Cheung, R. Mak, J. Schaack, G. S. Feng, N. W. Chi, J. M. Olefsky, and J. Shao. 2014. C/EBPα regulates macrophage activation and systemic metabolism. *Am. J. Physiol. Endocrinol. Metab.* 306: E1144–E1154.
70. Uematsu, S., T. Kaisho, T. Tanaka, M. Matsumoto, M. Yamakami, H. Omori, M. Yamamoto, T. Yoshimori, and S. Akira. 2007. The C/EBPβ isoform 34-kDa LAP is responsible for NF-IL-6-mediated gene induction in activated macrophages, but is not essential for intracellular bacteria killing. *J. Immunol.* 179: 5378–5386.
71. Pizarro-Cerdá, J., M. Desjardins, E. Moreno, S. Akira, and J. P. Gorvel. 1999. Modulation of endocytosis in nuclear factor IL-6$^{-/-}$ macrophages is responsible for a high susceptibility to intracellular bacterial infection. *J. Immunol.* 162: 3519–3526.
72. Davies, L. R., O. M. Pearce, M. B. Tessier, S. Assar, V. Smutova, M. Pajunen, M. Sumida, C. Sato, K. Kitajima, J. Finne, et al. 2012. Metabolism of vertebrate amino sugars with *N*-glycolyl groups: resistance of α2–8-linked *N*-glycolylneuraminic acid to enzymatic cleavage. *J. Biol. Chem.* 287: 28917–28931.
73. van der Poll, T., M. Levi, S. J. van Deventer, H. ten Cate, B. L. Haagmans, B. J. Biemond, H. R. Büller, C. E. Hack, and J. W. ten Cate. 1994. Differential effects of anti-tumor necrosis factor monoclonal antibodies on systemic inflammatory responses in experimental endotoxemia in chimpanzees. *Blood* 83: 446–451.
74. van Deventer, S. J., H. R. Büller, J. W. ten Cate, L. A. Aarden, C. E. Hack, and A. Sturk. 1990. Experimental endotoxemia in humans: analysis of cytokine release and coagulation, fibrinolytic, and complement pathways. *Blood* 76: 2520–2526.
75. Redl, H., S. Bahrami, G. Schlag, and D. L. Traber. 1993. Clinical detection of LPS and animal models of endotoxemia. *Immunobiology* 187: 330–345.
76. Barreiro, L. B., J. C. Marioni, R. Blekhman, M. Stephens, and Y. Gilad. 2010. Functional comparison of innate immune signaling pathways in primates. *PLoS Genet.* 6: e1001249.
77. Sibley, C. G., and J. E. Ahlquist. 1984. The phylogeny of the hominoid primates, as indicated by DNA-DNA hybridization. *J. Mol. Evol.* 20: 2–15.
78. Patterson, N., D. J. Richter, S. Gnerre, E. S. Lander, and D. Reich. 2006. Genetic evidence for complex speciation of humans and chimpanzees. *Nature* 441: 1103–1108.

Supplementary Materials

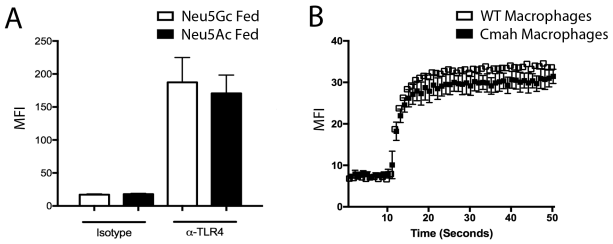

Supplementary Figure 1: Surface TLR4 Expression and Fluorescent LPS Binding Is Similar in WT and Cmah$^{-/-}$ Macrophages (A) Surface TLR4 expression of peritoneal macrophages isolated from WT and Cmah$^{-/-}$ mice (n=4). (B) Real time measurement of fluorescent LPS binding to macrophages present in the total peritoneal lavage from WT and *Cmah*$^{-/-}$ mice (n=4).

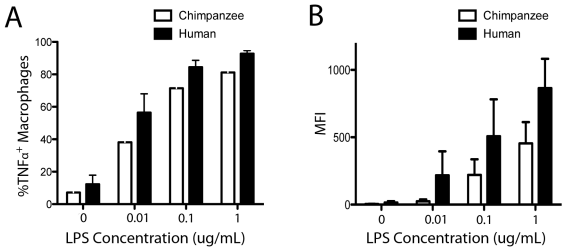

Supplementary Figure 2: Comparison of the Inflammatory Response in Human and Chimpanzee Monocytes Monocytes from humans and chimpanzees (n=6) were CD14 positively enriched and stimulated with LPS in the presence of Brefeldin A for 4 hours. (A) The %TNFα positive monocytes and (B) the median fluorescence intensity of intracellular TNFα were determined by flow cytometry.

Supplementary Figure 3: **Mouse and Human Macrophages Incorporate Neu5Gc After Feeding**

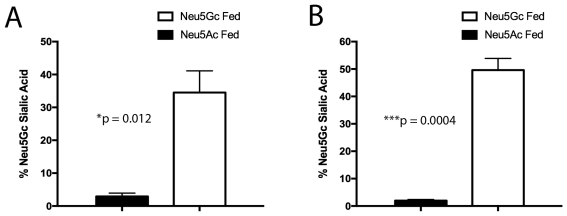

(A) Peritoneal macrophages from Cmah$^{-/-}$ mice were fed 2 mM Neu5Gc or Neu5Ac for 3 days (n=5). (B) Monocyte derived macrophages from humans were fed 2 mM Neu5Gc or Neu5Ac for 4 days during differentiation into macrophages. Sialic acid content was determined by DMB-HPLC.

Supplementary Table 1: Genes Are Significantly Differentially Expressed between Cmah$^{-/-}$ macrophages fed equal concentrations of either Neu5Ac or Neu5Gc

Gene	Mean Count	log2(Fold Change)	Standard Error log2 (Fold Change)	q value
Jund	2250	-0.558	0.0553	6.01E-20
Scand1	322	-0.954	0.108	5.75E-15
Crlf2	2200	-0.354	0.0628	0.0000627
Bri3	726	-0.694	0.124	0.0000627
Cebpb	1840	-0.548	0.106	0.000495
Bcl7c	109	-0.869	0.171	0.000495
Csf2ra	3780	-0.3	0.0593	0.000495
Fam20c	9130	-0.144	0.0284	0.000495
Map7d1	4550	-0.179	0.0355	0.000495
Ptms	3880	-0.243	0.0477	0.000495
Hnrnpa0	1190	-0.358	0.0744	0.00148
2310036O22Rik	1140	-0.301	0.0629	0.0016
H2afj	310	-0.624	0.136	0.00389
Dctn1	1970	-0.247	0.0549	0.00545
Sdf2l1	718	-0.316	0.0706	0.00574
Rnaseh2c	358	-0.413	0.0949	0.00904
Trim8	858	-0.297	0.0682	0.00904
Ehmt2	1850	-0.216	0.0507	0.0127
Ppp1r9b	2830	-0.309	0.0731	0.0133
Dhrsx	323	-0.586	0.139	0.0145
Slc15a3	21500	-0.195	0.0469	0.0165
B4galnt1	2200	-0.218	0.0532	0.0207
Heatr1	709	0.277	0.0678	0.0207
Zfp771	88	-0.83	0.204	0.0221
Atp13a2	3810	-0.278	0.0687	0.0227
Rps2	1580	-0.25	0.0619	0.0227
Ssbp4	961	-0.256	0.0641	0.0257
Zfp36l2	4670	-0.285	0.072	0.029
Kdm6b	409	-0.459	0.117	0.0333
Irf2bp2	1440	-0.279	0.0716	0.0352
Rnf44	1780	-0.248	0.0641	0.0398
Keap1	814	-0.276	0.0719	0.0422
Iscu	481	-0.313	0.0822	0.0447
Plxnd1	4120	-0.255	0.0667	0.0447
Tmsb4x	43100	0.101	0.0267	0.0455

Genes are displayed in order of significance (q value, determined by DESeq analysis).